Supplementary Information

Visual analysis of pyrophosphatase assisted by red and green two-color distance-reading test strips for diagnosis of hyperthyroidism

Tian Shi[a,b,#], Wu Peng[a,#], Li Yan[a], Maoyuan Zhao[a], Zixuan Zhan[a,*], Binwu Ying[a,*], Piaopiao Chen[a,*]

[a] Department of Laboratory Medicine, Med+X Center for Manufacturing, Department of Respiratory and Critical Care Medicine, Institute of Respiratory Health, Lung Cancer Center, Out-patient Department, National Clinical Research Center for Geriatrics, West China Hospital, Sichuan University, Chengdu, Sichuan, 610041, China

[b] Department of Laboratory Medicine, Minda Hospital of Hubei Minzu University, Enshi, Hubei, 445000, China

*Corresponding authors. E-mails: zxzhan@scu.edu.cn; yingbinwu@scu.edu.cn; chenpp0828@wchscu.cn.

[#]Tian Shi and Wu Peng contributed equally to this work.

Content

Materials and reagents.

All reagents used in this work were of analytical-reagent or higher grade and used without further purification. Pyrophosphatase (PPase, inorganic, from yeast), human serum albumin (HSA), lysozyme, transferrin, papain, cysteine, alanine, proline, valine, lysine, α-$_L$-fucosidase (AFu), mucin 1, thrombin, alkaline phosphatase (ALP), and NaF were obtained from Sigma-Aldrich Co.; Ltd. (China). Sodium pyrophosphate (PPi), hydrochloride (HCl), glucose, urea, creatinine, NaOH, NaCl, KCl, $MgCl_2$, $MnCl_2$, $NiCl_2$, $ZnCl_2$, $CaCl_2$, $BaCl_2$, $CoCl_2$, $FeCl_2$, $SnCl_2$, $AlCl_3$, $Ce(NO_3)_3$, $FeCl_3$, $CrCl_3$, Na_3PO4, KH_2PO4, 1 M Tris-HCl solution (pH 7.4, sterile), and $CuCl_2$ used in this work were obtained from Shanghai Sangon Biological Engineering Technology and Services Co.; Ltd. (China). Cadmium chloride ($CdCl_2{\cdot}2.5H_2O$), sodium tellurite (Na_2TeO_3), and potassium borohydride (KBH_4) were purchased from Kelong Chemical Reagents (Chengdu, China). $AgNO_3$, 3-mercaptopropionic acid (MPA) were obtained from Aladdin Reagent Co.; Ltd (Shanghai, China). Human serum samples were donated from the West China Hospital of Sichuan University (Chengdu, China, approval number: 20191045). All solutions were stored at 4 °C in a refrigerator until use.

Instruments.

The absorption and fluorescence spectrum of probe and CdTe QDs were recorded by the Duetta Spectrophotometer (HORIBA Canada Inc). High-resolution

transmission electron microscope (HR-TEM) measurements of CdTe QDs, Cu^{2+} + QDs, PPi-Cu^{2+}-PPi + QDs were carried out by a Tecnai G2F20 STWIN TEM at an accelerating voltage of 200 kV (FEI Co.; USA). ^{1}H nuclear magnetic resonance (NMR), ^{13}C NMR spectra were measured on a Bruker AM400 NMR spectrometer. Proton Chemical shifts of NMR spectra were given in ppm relative to internals reference TMS (^{1}H, 0.00 ppm). High resolution mass spectrum (HR-MS) spectral data were recorded on a Bruke Daltonics Bio TOF mass spectrometer. Lifetime analysis of probe and probe with PPase were recorded by Fluorolog-3 spectrometer (Horiba Jobin Yvon, France). Chromatographic paper without fluorescence (12 × 13 cm, Whatman, UK) was printed out by ink-jet printer (HP Deskjet 1112) in the shape of test strips with CdTe QDs stock solution. Fourier transform infrared (FTIR) spectra of Probe-Cu^{2+} and QDs were measured on a Nicolet IS10 FTIR spectrometer (Thermo Inc., America). Calibration of solution pH was used by PHS-2F pH Meter (INESA Co., Ltd, China).

Synthesis of CdTe QDs.

The CdTe QDs were synthesized referring to the previously reported method [1-3]. Firstly, a 50 mL solution containing $CdCl_2$ (0.5 mmol) and trisodium citrate (0.2 g) was prepared. Then, MPA (52 μL) was instantly added into the above solution, and the solution pH was adjusted to 10.5 with NaOH. Later, Na_2TeO_3 (0.1 mmol) and KBH_4 (50 mg) were added into the above solution, and refluxed for 1 h to obtain the CdTe QDs. Subsequently, high purity CdTe QDs were obtained via precipitating within-propanol and centrifuging (11000 rpm). The purified red CdTe QDs were

redispersed in high purity water before use.

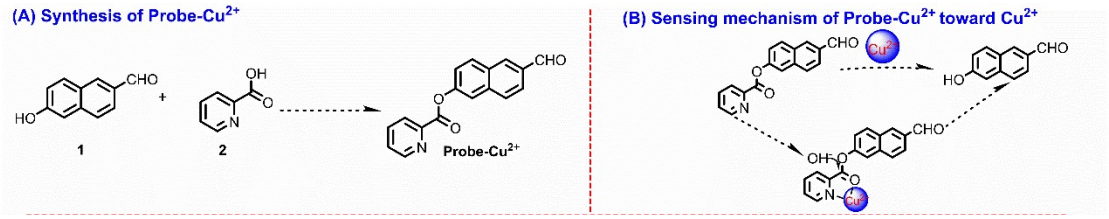

Scheme S1. Synthesis of Probe-Cu^{2+} (A) and sensing mechanism of Probe-Cu^{2+} toward Cu^{2+} (B).

Synthesis of Probe-Cu^{2+}.

A solution of 6-hydroxy-2-naphthaldehyde (172 mg, 1.0 mmol) in anhydrous dichloromethane (DCM, 10 mL) was treated with 2-picolinic acid (183.2 mg, 1.5 mmol), 1-Ethyl-3-(3-dimethylaminopropyl) carbodiimide (EDCI, 287.6 mg, 1.5 mmol), and 4-Dimethylaminopyridine (DMAP, 73.3 mg, 0.6 mmol). The resultant solution was stirred at room temperature for 2 h. After completion of the reaction, the reaction was diluted with water. The organic phase was separated, and the aqueous phase was extracted with DCM. The organic phases were combined and washed with 0.1 mol/L hydrochloride (HCl), saturated brine, dried over anhydrous sodium sulfate. The solvents were evaporated to give crude solid, which was purified by silica gel column chromatography using petroleum ether/ethyl acetate = 4:1 - 2:1 as eluent to afford the desired product as a white solid. ^{1}H NMR (400 MHz, $CDCl_3$, ppm) 10.17 (s, 1H), 8.90 (d, J = 3.2 Hz, 1 H), 8.36 (m, 2 H), 8.09 (d, J = 8.8 Hz, 1 H), 7.98 (m, 3 H), 7.84 (s, 1 H), 7.63 (m, 1 H), 7.55 (s, 1 H). ^{13}C NMR (100 MHz, DMSO-*d6*, ppm) 163.44, 163.39, 142.84, 138.15, 133.02, 131.95, 131.78, 131.34, 130.24, 129.90, 129.49, 129.25, 128.87, 126.75, 123.34, 122.56. HR-ESI-MS, [M] = $C_{17}H_{11}NO_3$:

calcd: 278.0812, found: 278.0812 $[M + H]^+$.

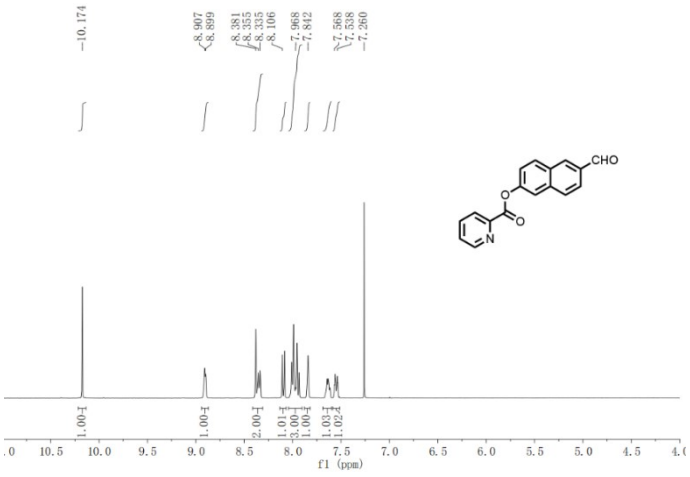

Fig. S1. ^{1}H NMR of **Probe-Cu^{2+}.**

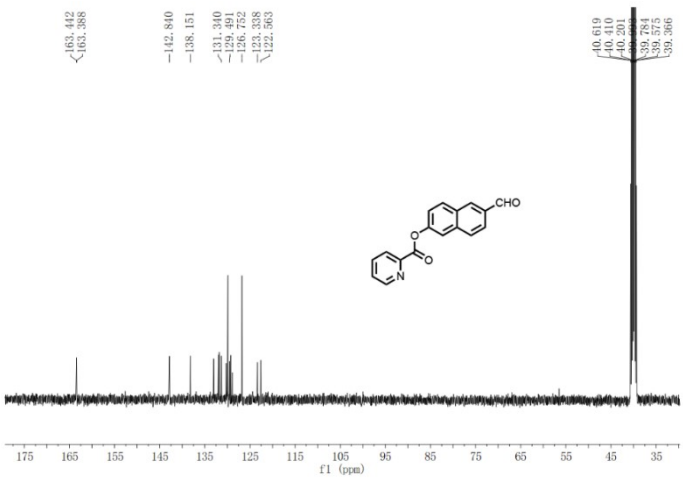

Fig. S2. ^{13}C NMR of **Probe-Cu^{2+}.**

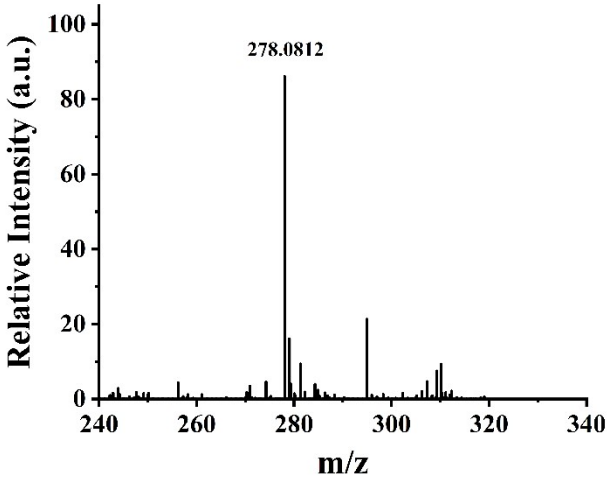

Fig. S3. HRMS of **Probe-Cu^{2+}**.

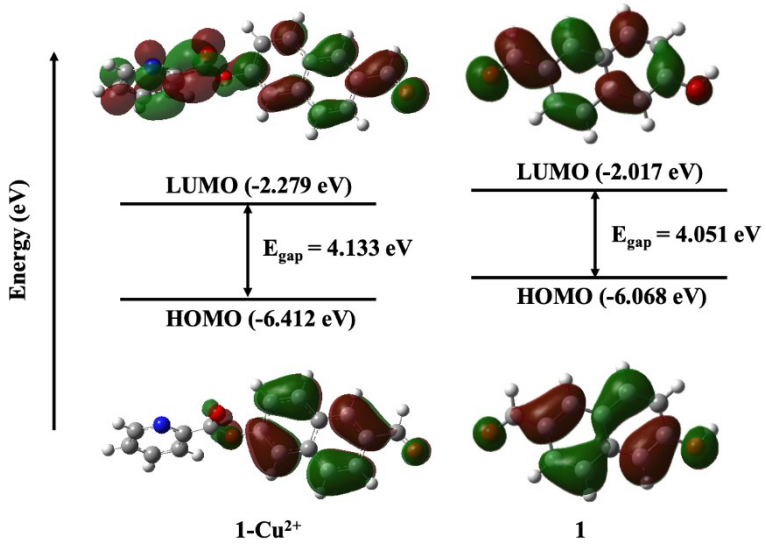

Fig. S4. The highest occupied molecular orbital-lowest unoccupied molecular orbital (HOMO-LUMO) energy levels of **Probe-Cu^{2+}** and **1**.

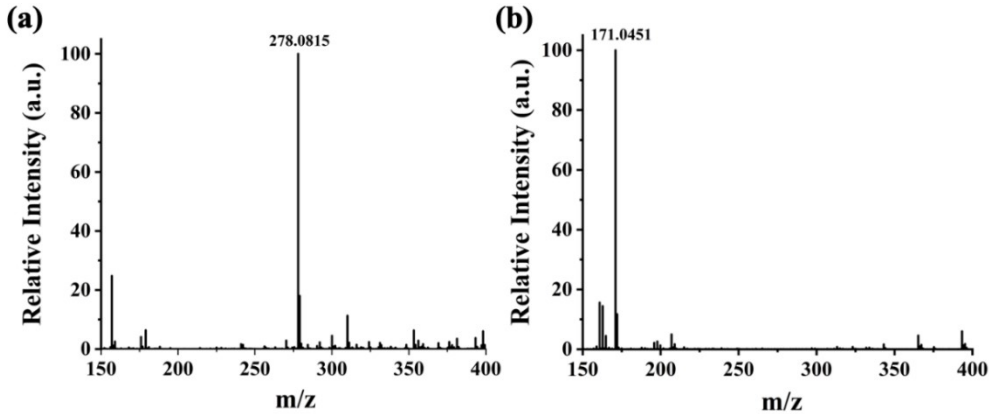

Fig. S5. The MS spectra of (a) **Probe-Cu^{2+}** (b) the reaction product between **Probe-Cu^{2+}** and Cu^{2+}.

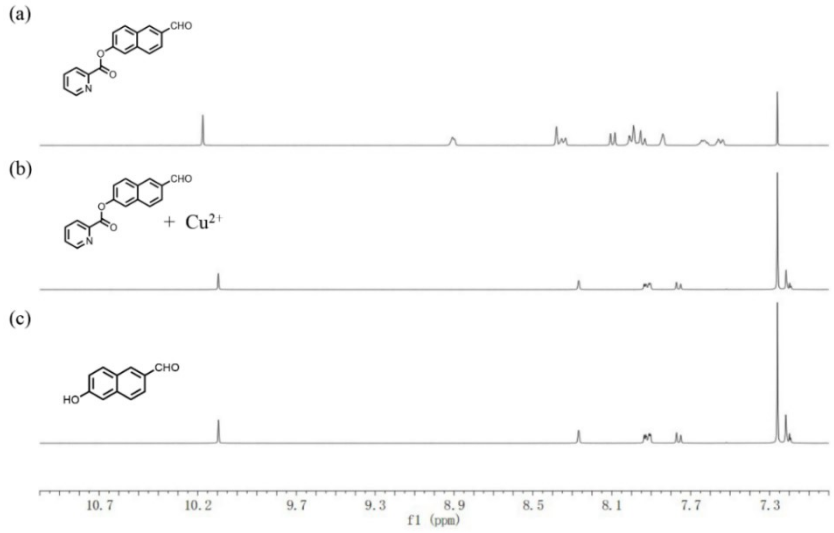

Fig. S6. ^{1}H NMR spectra of **Probe-Cu^{2+}** (a) the reaction product between **Probe-Cu^{2+}** and Cu^{2+} (b) compound **1** (c) in $CDCl_3$.

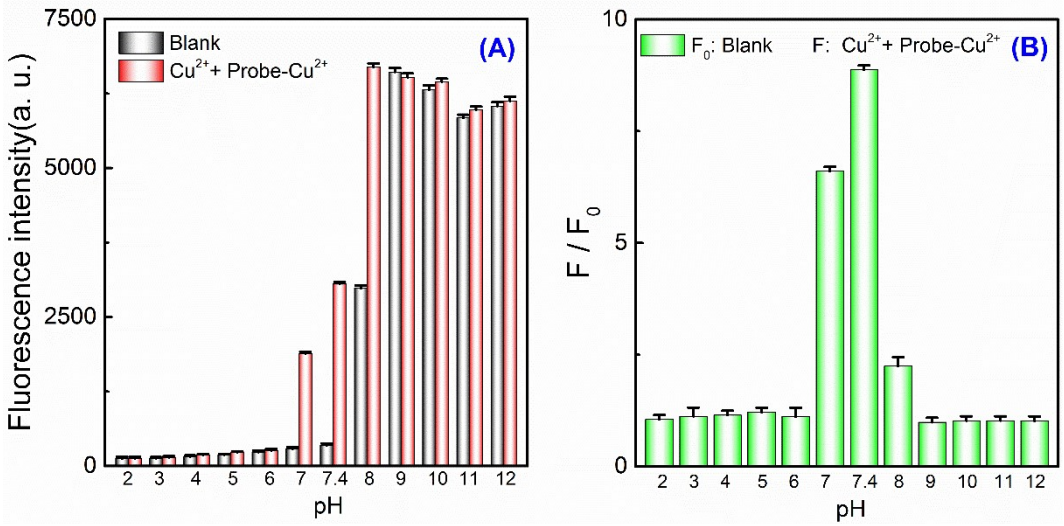

Fig. S7. Effect of pH on Probe-Cu^{2+} in recognition of Cu^{2+}. (A) The fluorescence intensity of Cu^{2+}+Probe-Cu^{2+} in pH 2-12 compared to the blank solution. (B) The fluorescence intensity of Cu^{2+}+Probe-Cu^{2+} (F) / blank solution (F_0) in pH 2-12. Error bars were estimated from three replicate measurements.

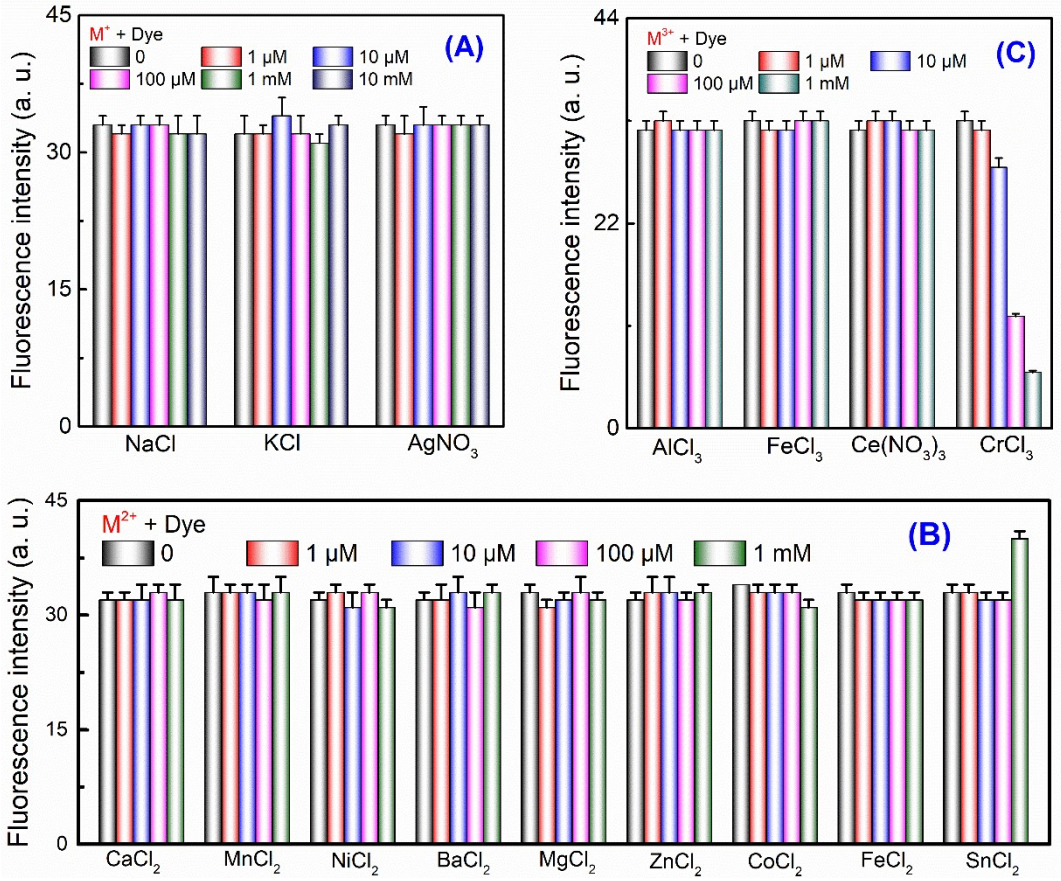

Fig. S8. The specificity of Probe-Cu^{2+} for Cu^{2+} recognition. The fluorescence emission wavelength at 520 nm. Error bars were estimated from three replicate tests.

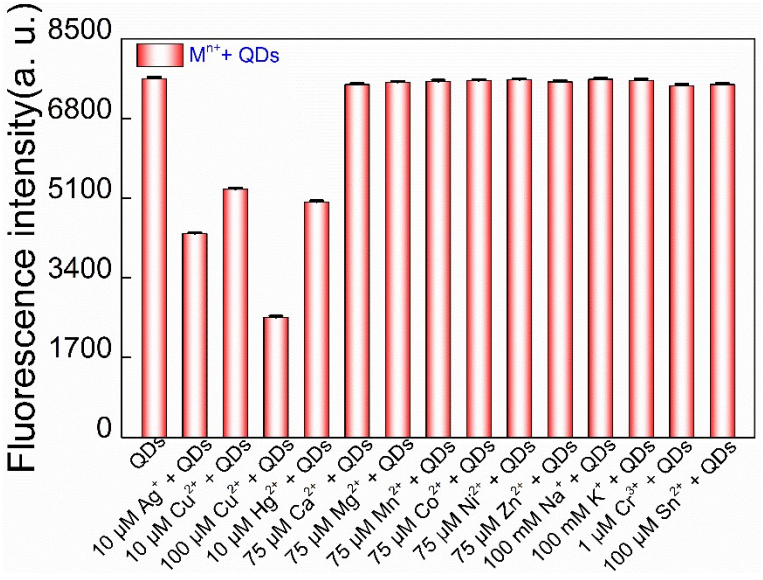

Fig. S9. The fluorescence intensity responses of CdTe QDs in the presence of various coexisting ions. The fluorescence emission wavelength at 694 nm (QDs). Error bars were estimated from three replicate tests.

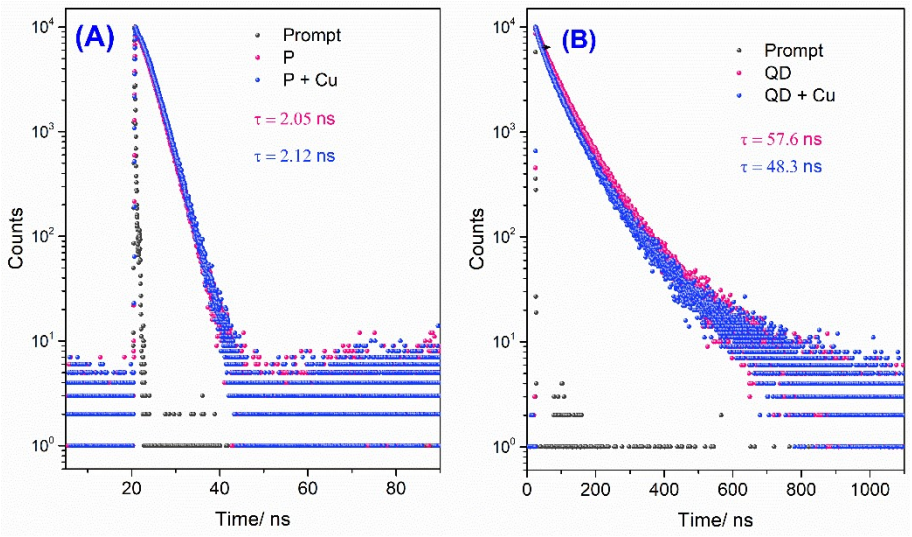

Fig. S10. The fluorescence lifetime of Probe-Cu^{2+} + Cu^{2+} (A), and QDs + Cu^{2+} (B).

Optimization of Conditions of PPase Analysis.

The experimental conditions were investigated to acquire the best quantitative sensitivity of PPase (Fig. S11). The concentration of PPi is a prerequisite for this detection system. At a PPi concentration of 20 mM, the dual signal reporters achieved the maximum and minimum fluorescence intensities for QDs and Probe-Cu^{2+}, respectively (Fig. S11A). Mg^{2+} was required for the activation of PPase. The concentration of Mg^{2+} for optimal catalytic hydrolysis of PPi was 20 mM (Fig. S11B). The reaction time of PPase to catalyze PPi and the coordination of Cu^{2+} with PPi also influenced the experiment's efficiency. The fluorescence signals of Probe-Cu^{2+} and QDs stabilized after 30 min (Fig. S11C and S11F). The maximum fluorescence difference was obtained at 100 μM Cu^{2+} (Fig. S11D and S11E), 24 μL Probe-Cu^{2+} (Fig. S11G and S11H), and 0.5 μL QDs (stock solution, Fig. S11J and S11K), respectively. The fluorescence signals of Probe-Cu^{2+} increased as the reaction time increased and remained stable for 6 min (Fig. S11I). In contrast, the fluorescence

signals of QDs decreased and remained stable for 6 min (Fig. S11L). In conclusion, the following conditions were deemed best for the subsequent detection of PPase: 20 mM PPi, 20 mM Mg^{2+}, 100 μM Cu^{2+}, 24 μL Probe-Cu^{2+}, 0.5 mL QDs, 30 min for PPase to catalyze PPi, 30 min for PPi-Cu^{2+}-PPi complex, 6 min for cation exchange reaction (CER) and Cu^{2+} coordination with PPi.

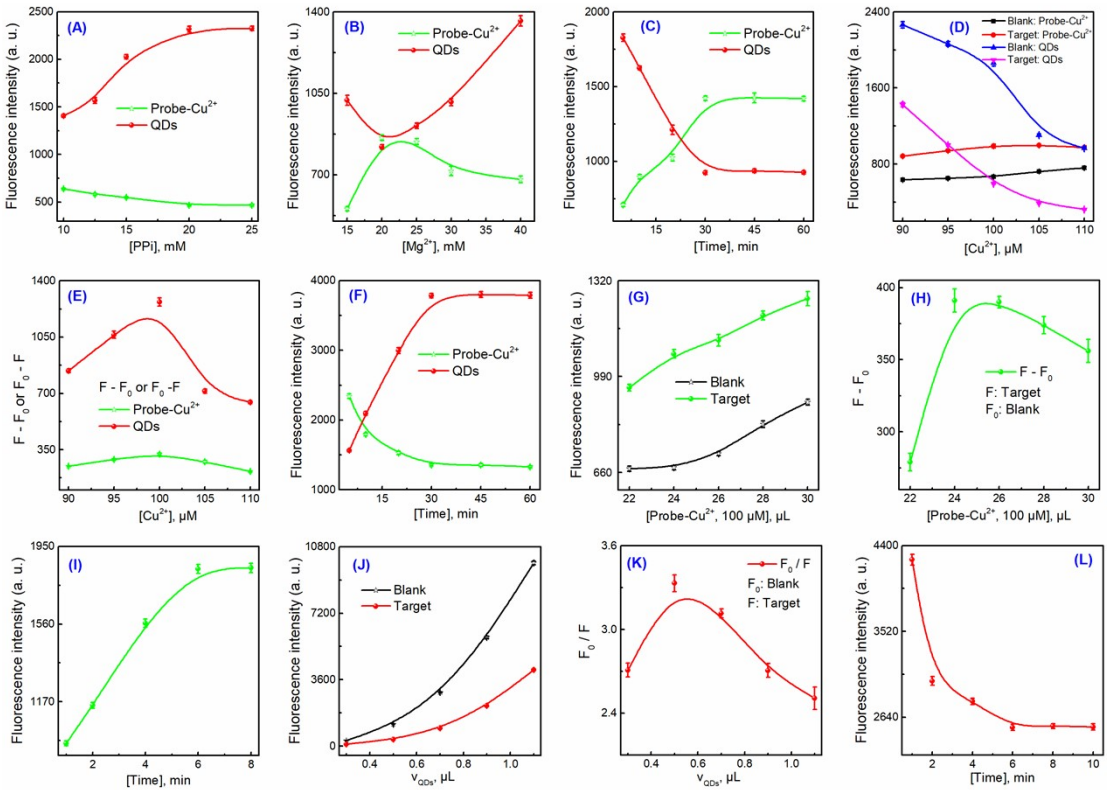

Fig. S11. Optimization of conditions of PPase analysis. (A) Concentration of PPi. (B) Concentration of Mg^{2+}. (C) Time for PPase to hydrolyze PPi. (D, E) Concentration of Cu^{2+}. (F) Complexing time between Cu^{2+} and PPi. (G, H) Concentration of Probe-Cu^{2+}. (I) Time for Cu^{2+} to hydrolyze Probe-Cu^{2+}. (J, K) Amount of QDs. (L) Time of CER. Error bars taken from three repeated tests. Blank is 0 U/L, target is 100 U/L PPase. The fluorescence emission wavelengths at 520 nm (Probe-Cu^{2+}) and 694 nm (QDs).

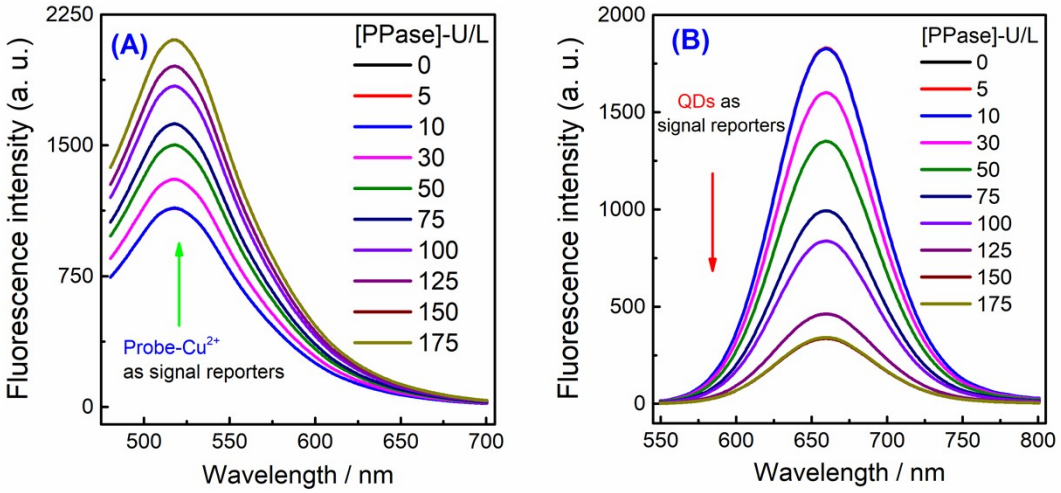

Fig. S12. Fluorescence emission of Probe-Cu^{2+} (A) and QDs (B) under different concentration of PPase, respectively.

Manufacture of Probe-Cu^{2+} and QDs-Based Test Strips

The Probe-Cu^{2+} and QDs-based test strips were manufactured using dip-dying and ink-jet printing, respectively. As the probe-Cu^{2+} is fat soluble, it is soluble in the organic solvent. For safety, it cannot be printed by inkjet like QDs, but made by dip-dying. Chromatographic paper without fluorescence (12 × 13 cm, Whatman, UK) was used for making test strips. For Probe-Cu^{2+}-based test strips, chromatography paper was soaked for 3 s in Probe-Cu^{2+} solution (100 μM). For QDs-based test strips, chromatography paper was printed out by an ink-jet printer in the shape of test strips with CdTe QDs stock solution. The samples were then air-dried, and sliced into test strips (7.5 cm × 3 mm).

Analysis Steps of PPase using Test Strips

Briefly, 50 μL of varying concentrations of PPase, and 10 μL PPi (20 mM) were added into 78 μL Tris-HCl (10 mM, 500 mM NaCl, 20 mM $MgCl_2$, pH 7.4) and

incubated at 37 ℃ for 0.5 h to complete the hydrolysis reaction and generate Pi. Subsequently, 10 μL Cu^{2+} (100 μM) was mixed and incubated at 37 ℃ for 0.5 h to generate the PPi-Cu^{2+}-PPi complex. Then, the Probe-Cu^{2+} and QDs-based test strip were vertically inserted into the test tube for 50 s. Finally, the diffusion distance of test strips was measured under ultraviolet light.

Probe-Cu^{2+} and QDs-based test strips were used as the signal reporters. The enhanced and quenching distances were longer and showed linear relationships with increased PPase concentrations (Fig. S13A and S13B). It showed good linearity in the PPase concentration range of 10-150 U/L. The linear equation of Probe-Cu^{2+} and QDs were D = 0.009C + 3.72 and D = 0.0065C + 3.78, respectively.

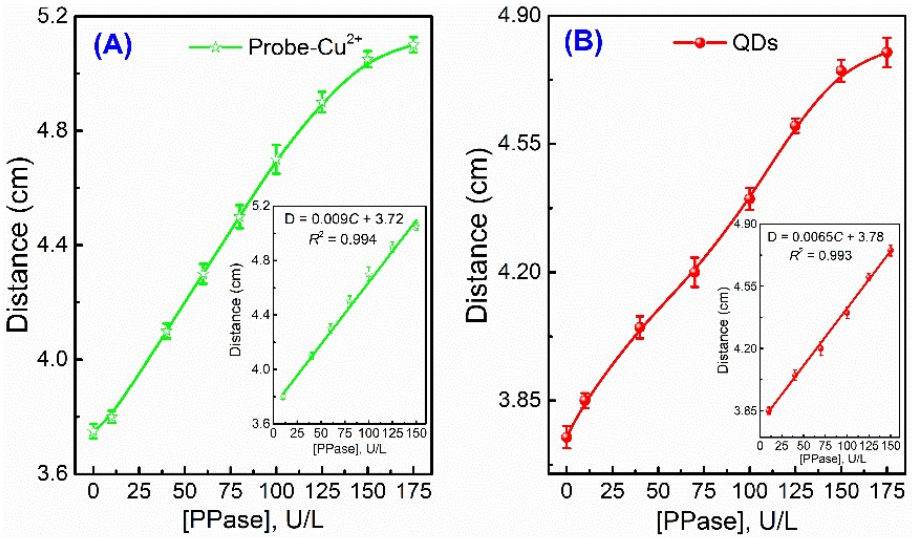

Fig. S13. Standard curves between the diffusion distance and the PPase using Probe-Cu^{2+} (A) and QDs (B) as signal reporters, respectively. Error bars were estimated from three replicate tests.

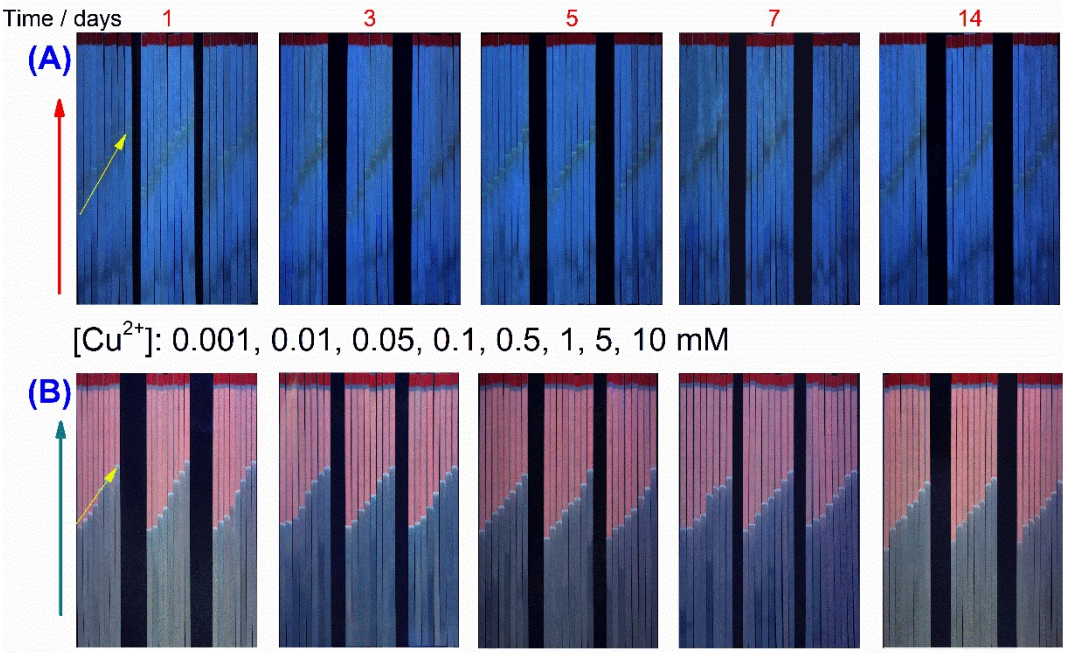

Fig. S14. Stability and repeatability of Cu^{2+}-Probe and QDs test strips. The distance reading test strips were measured three times repeatedly.

Table S1. Comparison of different methods for the determination of PPase

Method	Signal reporters	System	Linear range; LOD	Reaction time, min	Homogeneous	Visual	Verify practicality	Reference
Fluorescence	Single	Au NCs[c]	1-20 mU/L;1 mU/L	80	Yes	No	diluted 3T3L1 cell lysate (10%)	[4]
Fluorescence	Single	Au/Ag NCs[d]	1-30 U/L; 0.3 U/L	80	Yes	Yes	Spiked human serum samples	[5]
Fluorescence	Single	Cu NCs[e]	3-40 U/L; 1.3 U/L	90	Yes	No	Fresh rat serum samples	[6]
ECL[a]	Single	Click chemistry and HCR[b]	0.025-50 mU/L; 8 μU/L	140	No	No	Diluted arthritic patient serum-recovery	[7]
Fluorescence/ Visual	Two	PPi-Ce CPNs[f]; QDs; Cu^{2+}	1-25 U/L and 5-125 U/L; 0.15 and 0.8 U/L	72	Yes	Yes	Serum from patients with hyperthyroidism	[8]
Binary visual	Two	Probe-Cu^{2+}, QDs, Cu^{2+}-PPi	10-125 U/L, 3 U/L	72	Yes	Yes	Serum from patients with hyperthyroidism	This work

[a] Electrochemiluminescence; [b] hybridization chain reaction; [c] gold nanoclusters; [d] Au/Ag nanoclusters; [e] Cu nanoclusters; [f] pyrophosphate–cerium coordination polymeric nanoparticles.

Table S2. PPase concentration of serum samples (U/L)

No.	Clinical diagnosis	TSH[a]	FT3[b]	FT4[c]	PPase	No.	Clinical diagnosis	TSH[a]	FT3[b]	FT4[c]	PPase

1	Non-hyperthyroidism	2.62	4.8	14.0	333	38	Non-hyperthyroidism	1.11	4.4	16.4	226
2	Non-hyperthyroidism	1.27	5.9	17.9	472	39	Non-hyperthyroidism	2.43	5.0	14.9	256
3	Non-hyperthyroidism	2.06	4.7	16.3	436	40	Non-hyperthyroidism	2.42	4.0	14.3	382
4	Non-hyperthyroidism	2.40	4.7	19.8	318	41	Non-hyperthyroidism	1.57	4.5	14.7	91
5	Non-hyperthyroidism	1.75	5.2	15.8	279	42	Non-hyperthyroidism	1.26	4.6	15.4	170
6	Non-hyperthyroidism	1.75	5.2	16.8	390	43	Non-hyperthyroidism	2.05	4.9	16.6	408
7	Non-hyperthyroidism	1.88	6.1	18.4	342	44	Hyperthyroidism	<0.005	NM[d]	43.5	862
8	Non-hyperthyroidism	3.35	5.0	13.2	367	45	Hyperthyroidism	0.005	10.4	36.1	900
9	Non-hyperthyroidism	3.14	4.8	14.6	323	46	Hyperthyroidism	<0.005	29.6	61.2	837
10	Non-hyperthyroidism	4.02	4.9	14.4	214	47	Hyperthyroidism	<0.005	19.5	48.5	702
11	Non-hyperthyroidism	2.13	5.1	18.2	455	48	Hyperthyroidism	<0.005	23.4	46.0	712
12	Non-hyperthyroidism	2.08	6.2	16.8	229	49	Hyperthyroidism	0.077	38.8	69.1	821
13	Non-hyperthyroidism	4.07	4.5	13.8	435	50	Hyperthyroidism	<0.005	40.3	>100.0	600
14	Non-hyperthyroidism	0.99	4.8	16.5	358	51	Hyperthyroidism	<0.005	31.4	>100.0	560
15	Non-hyperthyroidism	2.67	4.0	12.1	320	52	Hyperthyroidism	<0.005	17.4	41.3	760
16	Non-hyperthyroidism	1.74	5.5	14.7	126	53	Hyperthyroidism	<0.005	33.2	>100.0	837
17	Non-hyperthyroidism	1.93	4.9	16.5	329	54	Hyperthyroidism	<0.005	NM	37.9	739
18	Non-hyperthyroidism	3.96	5.3	19.3	279	55	Hyperthyroidism	<0.005	17.6	46.7	725
19	Non-hyperthyroidism	1.63	5.1	15.9	388	56	Hyperthyroidism	<0.005	20.3	97.5	583
20	Non-hyperthyroidism	2.02	5.0	17.7	305	57	Hyperthyroidism	<0.005	NM	>100.0	648
21	Non-hyperthyroidism	1.05	4.5	18.2	76	58	Hyperthyroidism	<0.005	27.0	68.3	775
22	Non-hyperthyroidism	2.52	5.4	12.6	156	59	Hyperthyroidism	<0.005	27.6	81.0	527
23	Non-hyperthyroidism	2.83	5.9	17.0	211	60	Hyperthyroidism	<0.005	27.5	53.9	1648
24	Non-hyperthyroidism	1.54	5.2	15.3	135	61	Hyperthyroidism	<0.005	NM	53.0	1200
25	Non-hyperthyroidism	2.52	4.2	17.4	20	62	Hyperthyroidism	0.006	11.4	11.4	1857
26	Non-hyperthyroidism	3.51	4.6	16.2	13	63	Hyperthyroidism	0.051	14.3	45.4	1209
27	Non-hyperthyroidism	1.57	4.3	15.8	35	64	Hyperthyroidism	<0.005	12.9	30.8	1044
28	Non-hyperthyroidism	0.63	4.7	21.4	11	65	Hyperthyroidism	0.018	9.5	35.9	1290
29	Non-hyperthyroidism	1.09	4.9	16.3	132	66	Hyperthyroidism	<0.005	29.5	70.6	1104
30	Non-hyperthyroidism	1.94	5.4	14.8	223	67	Hyperthyroidism	<0.005	12.5	27.7	1017
31	Non-hyperthyroidism	2.28	4.7	16.2	276	68	Hyperthyroidism	<0.005	NM	94.2	1010
32	Non-hyperthyroidism	2.01	4.6	14.6	164	69	Hyperthyroidism	<0.005	NM	36.4	848
33	Non-hyperthyroidism	2.97	5.7	16.5	153	70	Hyperthyroidism	<0.005	15.7	NM	1465
34	Non-hyperthyroidism	1.01	6.8	18.7	370	71	Hyperthyroidism	<0.005	46.9	>100.0	1163
35	Non-hyperthyroidism	2.80	4.4	18.0	206	72	Hyperthyroidism	<0.005	27.1	95.0	925
36	Non-hyperthyroidism	2.18	4.4	16.9	470	73	Hyperthyroidism	<0.005	26.1	60.3	1008
37	Non-hyperthyroidism	1.62	4.9	15.5	206						

[a] Thyroid stimulating hormone (TSH, 0.27-4.2 mU/L); [b] free triiodothyronine 3 (FT3, 3.60-7.50 pmol/L); [c] free triiodothyronine 4 (FT4, 12.0-22.0 pmol/ L); [d] not mentioned.

References

1 P. P. Chen, Y. J. Bai, S. Y. Tang, N. Wang, Y. Q. He, K. Huang, J. Huang, B. W. Ying and Y. Cao,

Nano Lett., 2022, **22**, 1710-1717.

2 P. P. Chen, Y. Q. He, T. Y. H. Liu, F. L. Li, K. Huang, D. Tang, P. J. Jiang, S. J. Wang, J. Zhou, J. Huang, Y. Xie, Y. G. Wei, J. Chen, W. Hu and B. W. Ying, *Biosens. Bioelectron.*, 2022, **202**, 114009.

3 P. P. Chen, Y. Wang, Y. Q. He, K. Huang, X. Wang, R. H. Zhou, T. Y. H. Liu, R. L. Qu, J. Zhou, W. Peng, M. Li, Y. J. Bai, J. Chen, J. Huang, J. Geng, Y. Xie, W. Hu and B. W. Ying, *ACS Nano*, 2021, **15**, 11634-11643.

4 J. Sun, F. Yang, D. Zhao and X. R. Yang, *Anal. Chem.*, 2014, **86**, 7883-7889.

5 Z. L. Lei, J. Zhou, M. Liang, Y. Xiao and Z. H. Liu, *Front. Bioeng. Biotechnol.*, 2021, 1530.

6 M. S. Ye, Y. Yu, B. X. Lin, Y. Cai, Y. J. Cao, M. L. Guo and D. B. Zhu, *Sens. Actuators B Chem.*, 2019, **284**, 36-44.

7 X. C. Huang, J. P. Jia, Y. Lin, B. Qiu, Z. Y. Lin and H. X. Chen, *ACS Appl. Mater. Interfaces*, 2020, **12**, 34716-34722.

8 P. P. Chen, R. L. Qu, W. Peng, X. Wang, K. Huang, Y. Q. He, X. L. Zhang, Y. M. Meng, T. Y. H. Liu, J. Chen, Y. Xie, J. Huang, Q. Hu, J. Geng and B. W. Ying, *J. Mater. Chem. C*, 2021, **9**, 4141-4149.